Nanostructured Stable Floating M-Mono- and Bilayers and Langmuir-Schaefer Films of 5,10,15-Triphenylcorrole

Larissa A. Maiorova, Thao T. Vu, Olga A. Gromova, Konstantin S. Nikitin & Oskar I. Koifman

BioNanoScience

ISSN 2191-1630

BioNanoSci.
DOI 10.1007/s12668-017-0424-0

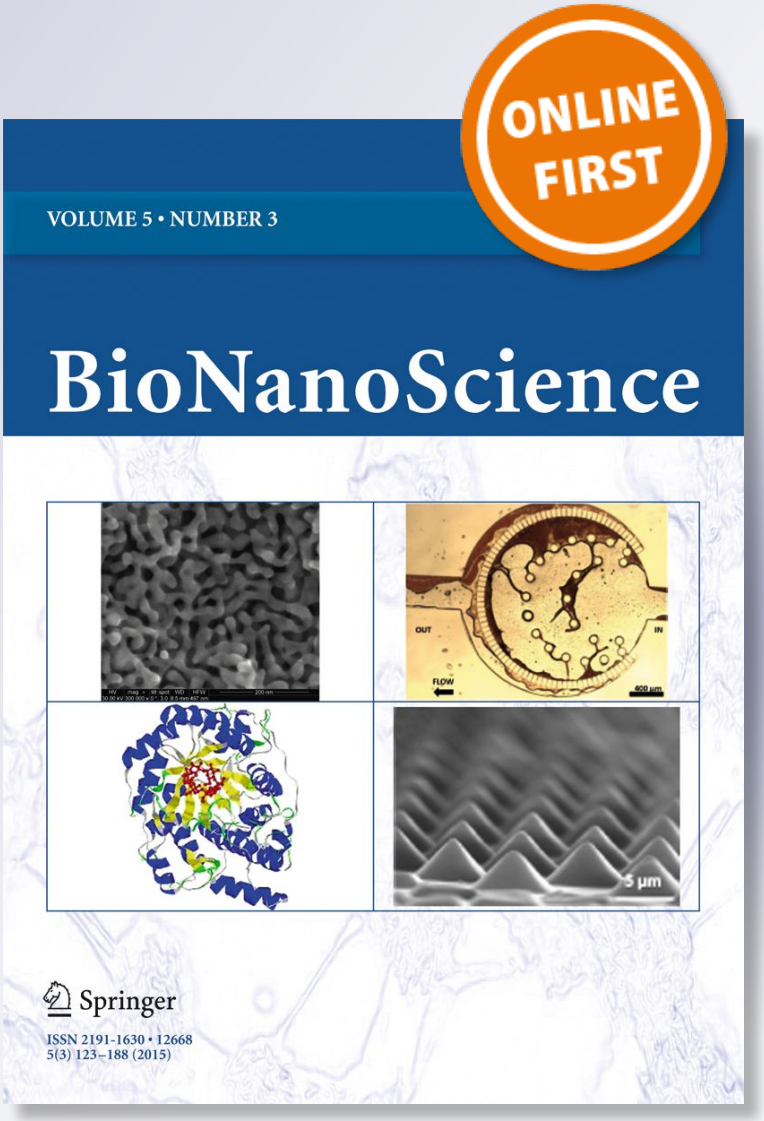

Springer

BioNanoSci.
DOI 10.1007/s12668-017-0424-0

Nanostructured Stable Floating M-Mono- and Bilayers and Langmuir-Schaefer Films of 5,10,15-Triphenylcorrole

Larissa A. Maiorova[1] · **Thao T. Vu**[1] · **Olga A. Gromova**[2] · **Konstantin S. Nikitin**[1] · **Oskar I. Koifman**[1,3]

Abstract 5,10,15-Triphenylcorrole is a tetrapyrrolic macrocyclic compound similar to B12 vitamin, with pyrrole-pyrrole direct coupling and a carbon skeleton. Stable floating nanostructured mono-, bi-, and tetralayers of the compound were prepared. The main characteristics of the structure, properties, and formation conditions of the layers were determined. A model of monolayers consisting of nanoaggregates was built. The triphenylcorrole produces nanostructured face-on and edge-on monolayers. Stable bilayers and tetralayers form at high values of the initial surface coverage, featuring a constant degree of surface coverage by 3D nanoaggregates at the initial point of the stable state (75%). The layers with bilayered 3D nanostructures demonstrate very high stability. Their size (8 nm) and the number of molecules in them (109) are independent of the initial degree of surface coverage. For the first time, a model of floating bilayers of a macroheterocyclic compound was constructed. Langmuir-Schaeffer films of the corrole were prepared from nanostructured floating polylayers produced on the water surface and then were studied spectrally.

Keywords Air-water interface · 2D and 3D nanostructures · Stable bilayers · Langmuir-Schaefer films · *J*-aggregates · Triphenylcorrole

✉ Larissa A. Maiorova
valkovala@mail.ru

[1] Research Institute of Macroheterocyclic Compounds, Ivanovo State University of Chemistry and Technology (ISUCT), 7 Sheremetevskii prosp, 153000 Ivanovo, Russia

[2] Ivanovo State Medical Academy, Ministry of Health of Russia, 8 Sheremetevskii prosp, 153000 Ivanovo, Russia

[3] Institute of Solution Chemistry, Russian Academy of Sciences, 1 ul. Akademicheskaya, 153045 Ivanovo, Russia

1 Introduction

Recently, there has been an increase in the number of studies focused on synthesizing and analyzing the structure, properties, and use of porphyrinoids (H_nPn) as analogues of porphyrins. Some practical properties of H_nPn and their metal complexes (MPn), such as catalytic and sensory activity, photodynamic characteristics, and nanostructuring capability, exceed those of porphyrin complexes [1–12]. Porphyrinoids are H_2P analogues, possessing a cyclic oligopyrrolic structure and normally distinguished by the type and size of the macrocycle's coordination center, as well as by the number and type of meso-bridges in it. The compounds in question have some peculiar and useful practical properties: an asymmetrical polarized structure of π-chromophore, selectivity of acid-base center, and metal coordination capability of the macrocycle, as well as a tendency towards stabilization of various oxidation degrees of metals within complexes, and formation of strong intra- and intermolecular hydrogen bonds [13].

The properties of systems obtained using the Langmuir-Blodgett technique largely depend on their state (which includes the characteristics of aggregation) in all the stages of the deposition process: solution, floating layer, and LB film [14–20]. Metalloporphyrinoids with a narrow coordination cavity (corroles) can be used for production of nanostructured layers [21]. The Langmuir-Blodgett method is applied to obtain porphyrinoid films with a given structure and thickness in a nanometer range [22–25]. However, managing molecule self-organization processes in films on solid substrates requires knowledge of individual conditions for film formation. In our previous studies, we demonstrated that the supramolecular design at the air-water interface with controlled self-assembly of organic compounds in 2D and 3D nanostructures becomes possible if one has quantitative information on the structure of the floating layer [26–30]. It was shown that major two-

Published online: 01 July 2017

dimensional aggregates sized 5–20 nm (M-nanoaggregates) are able to coalesce into larger nano- and microaggregates [22, 28]. Floating layers and thin Langmuir-Schaeffer (LS) films of corroles have been studied. The quantitative parameters of relationship between their structure and experimental conditions have been studied only with regard to the layers obtained using an extremely dilute solution of the compound [21]. However, low concentrations limit the possibility of 3D nanostructure formation at the water-air interface.

This study aims to obtain floating nanostructured 5,10,15-triphenylcorrole ($H_3(Ph)_3Cor$) M-mono- and polylayers, formed using relatively concentrated solution of the compound; determine their key characteristics and formation conditions; construct a model of floating mono- and polylayers; create a passport of floating layers; obtain LS films of $H_3(Ph)_3Cor$; and perform their spectral study.

2 Materials and Methods

5,10,15-Triphenylcorrole was synthesized by Thao T. Vu under the supervision of D.B. Berezin using a technique, described earlier [31]. Its structure was confirmed by NMR ^{1}N, IR, and UV-Vis spectra. The floating layers were obtained with a NT MDT Langmuir setup (Zelenograd, Russia) by applying the $H_3(Ph)_3Cor$ solution in methylene chloride ($C = 1.2 \times 10^{-4}$ M) onto the surface of bi-distilled water with microliter syringes (1, 10, 20, and 100 μl, "Hamilton", Sweden) at the temperature of 20 ± 1 °C. Layer compression with the speed of 2.3 cm^2 min^{-1} started 15 min after the application. Initial degrees of water surface coverage with corrole (c_{edge}) were varied from 2.7 to 58%. The surface pressure was measured by using a Wilhelmy plate with an accuracy of 0.02 mN m^{-1}. The error of measurement with respect to the surface area per molecule in the layer (A) was 2%. The A_{mol} values (surface area per molecule in an M-aggregate) and n (aggregation number) were determined by approximation of πA-π curve's portion with a linear function, by using the least squares technique (error $\pi A \leq 3\%$). The LS films were obtained by transferring the floating layer onto the quartz plate under conditions shown in Fig. 3a (point A). The electronic absorption spectra were registered with a UV/VIS Lambda 20 scanning spectrophotometer with ±0.1 nm wavelength setting accuracy. The reproducibility of the wavelength setting was ±0.05 nm, the photometric accuracy being ±0.003. The structure of the layers was analyzed by using quantitative analysis of compression isotherms of a nanostructured M-monolayer [32, 33]. The main characteristics of the floating layer were determined in the following manner: $\beta = kT/n$, where β is the ordinate of the intersection point between the line, describing the isotherm's πA-π region corresponding to the stable state of the layer, and the πA axis; A_{mol} is the line's tilt. According to the model being used, M-aggregate has a circular shape with the surface area of $S_{aggr} = A_{mol} \times n$ (nm^2) and the diameter of $D_{aggr} = \sqrt{4S_{aggr}/\pi}$ (nm). The layer's compressibility in a stable state can be defined as $B = \frac{A_i - A_f}{(\pi_f - \pi_i) \times A_i}$ (m/N), where π_i and π_f are the respective pressures at the start and at the end of the monolayer's stable state, with A_i and A_f being the abscissas of the start and the end of the linear portion of the π-A isotherm. The distance between the boundaries of the aggregates is the same on the average and can be calculated with the following relation: $d = \sqrt{\frac{4A_i \times n}{\pi}} - \sqrt{\frac{4A_{mol} \times n}{\pi}}$ (nm). The average distance between the molecules along the surface of the water (face-on) in an M_{face}-aggregate is $r = \sqrt{\frac{4A_{mol}}{\pi}} - \sqrt{\frac{4A_{proj}}{\pi}}$ (nm). The water coverage degrees at the initial point of the stable state can be defined as $c_{i\text{-face}} = A_{proj\text{-face}}/A_i$ 100% and $c_{i\text{-edge}} = A_{proj\text{-edge}}/A_i \times 100\%$, where $A_{proj\text{-face}}$ and $A_{proj\text{-edge}}$ are surface areas of face-on and edge-on projections of molecule models. Within the linear portion of the πA-π curve the tilt of the molecules (which have an anisotropic shape) in the stack of a compact non-aqueous aggregate can be defined as $\psi = \arcsin(A_{pack\text{-}edge}/A_{mol})$, where $A_{pack\text{-}edge}$ is the closest packed surface area. The content of water in M-aggregates (per molecule) and between them at the initial point of the stable state can be calculated as $w_{in\text{-}M} = A_{mol} - A_{proj}$ and $w_{inter\text{-}M\text{-}i} = A_i - A_{mol}$, respectively. The maximum error when defining characteristics of a layer is as follows: 3% for A_{mol} и $\Delta\pi$, 5% for c_{face} and ψ, 7% for D and $w_{inter\text{-}M\text{-}i}$, 10% for B, $c_{i\text{-face}}$, $c_{f\text{-face}}$, $c_{i\text{-edge}}$, $c_{f\text{-edge}}$, n, $w_{in\text{-}M}$, and d_i.

The geometric characteristics of the molecules and their closest packings were determined by constructing the corresponding molecular models (HyperChem 8.0.8, MM+ calculations). The surface areas of projections in case of face-on and edge-on positions of the molecules were found to be: $A_{proj(face)} = 1.6$ nm^2, $A_{proj(edge)} = 1.0$ nm^2; with the surface areas of the described rectangles being $A_{mod(face)} = 3.2$ nm^2 and $A_{mod(edge)} = 1.4$ nm^2, respectively (Fig. 1).

Surface areas, occupied by a molecule in a closest packed monolayer are $A_{pack(face)} = 1.9$ nm^2 and $A_{pack(edge)} = 1.2$ nm^2.

3 Results and Discussion

$H_3(Ph)_3Cor$ floating layers were formed from a solution in methylene chloride ($C = 1.2 \times 10^{-4}$ M) at layer compression speed of $v = 2.3$ cm^2/min. Structure analysis of floating layers was done with the method of quantitative analysis of compression isotherms (Fig. 2a, b), based on the Volmer equation, generalized to the case when structural units of 2D-gas are molecular aggregates rather than individual molecules. A single-phase state of a layer is described by the following equation: $\pi \cdot (A - A_{mol}) = n^{-1}kT$, where A_{mol} is the surface area per one molecule in a structure unit of a layer (a nanoaggregate); k is the Boltzmann constant; T is the absolute temperature; and n is the number of molecules in a

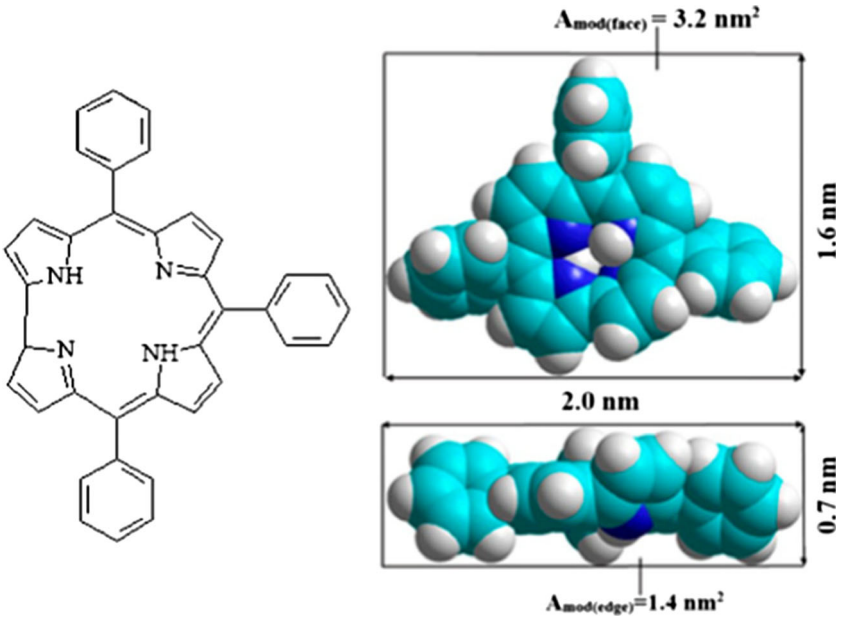

Fig. 1 Model of H_3Ph_3Cor molecule. A_{mod}—the surface areas of *circumscribed rectangles*

nanoaggregate (an aggregation number). The isotherms plotted in πA-π coordinates (Fig. 3a, b) comprise linear and nonlinear parts. The former corresponds to single-phase states, and the tangent of the slope angle of the linear part is equal to A_{mol}. The ratio of kT to the initial ordinate of the intersection of the axis and a straight line, whose segment approximates the linear part, is equal to n. Estimation of the structure is performed on the base of comparison of the A_{lim} value (limiting area at a curve section, preceding an inflection) and area values, calculated from the model of a molecule. A change in orientation of molecules with varying initial surface concentration N_0 is discussed with the use of values of initial surface coverage degrees c_{face} and c_{edge}: the ratios of the water surface area covered by molecules in face-on or edge-on orientation to the total water surface area prior the layer compression.

The analysis shows that stable mono-, bi-, and tetralayers of $H_3(Ph)_3Cor$ are formed on the water surface within the studied range of initial coverage degrees (c_{face}) from 4 to 30%. The main results of compression isotherm analysis and characteristics of $H_3(Ph)_3Cor$ floating layers are shown in Table 1. One can see that the corrole forms stable M-monolayers within a small range of the initial surface coverage degrees—c_{face} from 4.3 to 27.2% (Figs. 2 and 3, Table 1). At c_{face} ≥37.1%, polylayers form even at the lowest surface pressures.

The corrole forms stable monolayers of various types (Table 1). A face-on position of molecules (M_{face}) is found in nanoaggregates at c_{face} ≤10.9%, with edge-on position at 17.5% ≤c_{face} ≤ 27.2%. 3D nanoaggregates (bilayers—M_{bi}) are formed at 37.1% ≤c_{face} ≤ 61.9%, and if the initial surface coverage degree is further increased c_{face} ≥92.8% (c_{edge} ≥ 58.0%), then 3D nanoaggregates (tetralayers—M_{tetra}) are formed.

Lower c_{face} values (from 4.3 to 10.9%) result in the formation of monolayers with a face-on molecule position. Increasing c_{face} leads to increase of the aggregation number from 14 to 40 and decrease of the surface area per molecule (from 6.4 to 2.3 nm^2) and the distance between molecules in the aggregate (from 1.4 to 0.3 nm). Meanwhile, the aggregate's surface area (and diameter) remains unchanged at 95 nm^2 (11 nm). Monolayers with a face-on molecule position feature high water content in aqua-

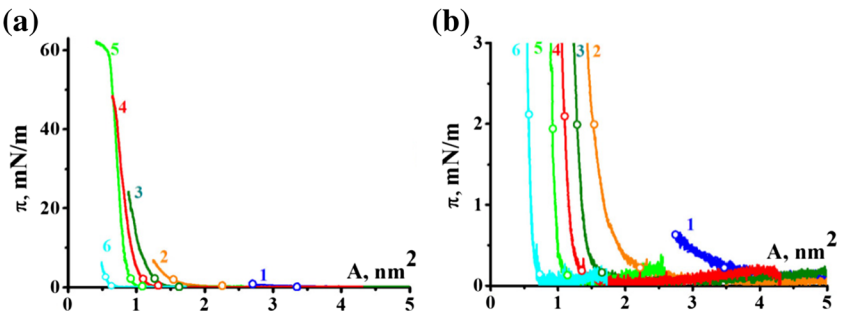

Fig. 2 π-A isotherms (**a**) and low-pressure range of the isotherms (**b**) of H3(Ph)3Cor, obtained at v = 2.3 cm^2/min and various initial surface coverage degrees. c_{face} = 10.9% (*1*), 17.5% (*2*), 27.2% (*3*), 37.1% (*4*), 61.9% (*5*), and 92.8% (*6*). $C = 1.2 \times 10^{-4}$ M (CH_2Cl_2). *Circles* denote the boundaries of the existence regions of the stable states of the layer

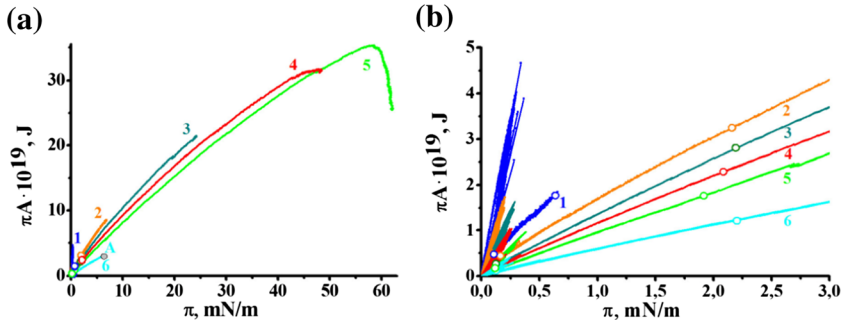

Fig. 3 πA-π isotherms (**a**) and low-pressure range of the isotherms (**b**) of H3(Ph)3Cor, obtained at v = 2.3 cm^2/min and various initial surface coverage degrees. c_{face} = 10.9% (*1*), 17.5% (*2*), 27.2% (*3*), 37.1% (*4*), 61.9% (*5*), and 92.8% (*6*). $C = 1.2 \times 10^{-4}$ M (CH_2Cl_2). The floating layers were transferred onto a solid support by dips at π_{tr} = 6 mN/m (*point A* on Fig.3a, layer state—"edge-on tetralayer-polylayer"). *Circles* denote the boundaries of the existence regions of the stable states of the layer

aggregates (up to 75% from A_{mol}) and between them (up to 3.0 nm^2 per single $H_3(Ph)_3Cor$ molecule).

At average degrees of initial surface coverage (c_{face} = 17.5–27.2%), the 0.1 to 2.2 mN/m pressure region forms stable edge-on monolayers, where the molecule's plane is tilted with respect to the water surface. The minimum inclination angle (ψ_{min}) of $H_3(Ph)_3Cor$ molecules in stacks varies from 55° to 66°, the number of molecules in M_{edge}-aggregates varying from 20 to 69. Unlike monolayers with face-on molecules, edge-on monolayers contain a small amount of water both inside (up to 18% per molecule when positioned vertically), and between (from 0.34 to 0.54 nm^2) nanoaggregates. Monolayer compressibility is from 100 to 140 m × N^{-1}.

It is characteristic of triphenylcorrole to form stable bilayers of 3D edge-on nanoaggregates which are tolerant to changes of the initial surface coverage degree (c_{face} from 37 to 62%) if the initial surface coverage degrees are high. They are formed within 0.1–2.2 mN/m pressure range. One of their main features is that the number of molecules in an aggregate (n = 109) and layer compressibility (B = 90 м × H^{-1}) do not depend on c_{face}.

At high initial surface coverage degrees ($c_{face} \geq 92.8\%$), a stable tetralayer (3D-nanoaggregates—M_{tetra}) with the number of molecules n = 202 is formed, the surface pressure being from 0.1 to 2.2 mN/m.

Our findings rendered it possible to build a quantitative model of $H_3(Ph)_3Cor$ floating M_{face}- and M_{edge}-monolayers, and M_{bi}-bilayers, formed from a solution in methylene chloride. Analyzing dependencies of the surface area per molecule in a nanoaggregate on the initial surface coverage degrees (Table 1, Fig. 4a) results in the following equations:

$$A_{mol} = -0.59 \times c_{face} + 8.79 \ (\text{for } M_{face} \text{ monolayers}) \quad (1)$$

$$A_{mol} = -0.016 \times c_{face} + 1.74 \ (\text{for } M_{edge} \text{ monolayers}) \quad (2)$$

$$A_{mol} = -0.01 \times c_{face} + 1.37 \ (\text{for } M_{bi}\text{3D}-\text{layers}) \quad (3)$$

The equations may facilitate determination of the constants characterizing a floating layer. As the minimum values of the surface area per molecule in a face-on monolayer (1.9 nm^2), edge-on monolayer (1.2 nm^2), and edge-on bilayer (0.6 nm^2) are known, the Eqs. (1–3) will provide the maximum initial surface coverage degrees (11.7, 33.8, and 77.0%, respectively) for maintaining these layer states. Taking into account the error when finding c_{face} values, the boundaries between the two states were determined: $c_{bord\_face\text{-}edge}$ = 12.1 ± 0.4%, $c_{bord\_edge\text{-}bi}$ = 34.8 ± 1.0%, $c_{bord\_bi\text{-}tetra}$ = 79.3 ± 2.4% (Fig. 4a).

Analyzing dependencies of other characteristics of stable layers on the initial surface coverage degree (Table. 1, Fig. 4b–f) results in the following equations:

For M_{face} monolayers:

$$n = -2 + 4 \times c_{face} \quad (4)$$

$$w_{in\text{-}M}/A_{mol} = 110.1\text{–}7.2 \times c_{face} \quad (5)$$

$$c_{i\text{–}face} = -2.8 + 4.5 \times c_{face} \quad (6)$$

$$r = 2.2\text{–}0.2 \times c_{face} \quad (7)$$

$$D_{aggr} = const \ (11 \text{ nm}) \quad (8)$$

$$c_{i\text{-}aggr} = const \ (75\%) \quad (9)$$

For M_{edge} monolayers:

$$n = -62 + 5 \times c_{face} \quad (10)$$

$$D_{aggr} = -2.3 + 0.5 \times c_{face} \quad (11)$$

$$w_{in\text{–}M}/A_{mol} = 36.8\text{–}1.0 \times c_{face} \quad (12)$$

$$w_{inter\ M\text{–}i} = 0.84\text{–}0.02 \times c_{face} \quad (13)$$

$$c_{i\text{–}edge} = 30.7 + 1.1 \times c_{face} \quad (14)$$

$$c_{f\text{–}edge} = 52.4 + 0.9 \times c_{face} \quad (15)$$

$$B = 184.0\text{–}3.1 \times c_{face} \quad (16)$$

$$\psi_{min} = 34.89 + 1.14 \times c_{face} \quad (17)$$

$$c_{i\text{–}aggr} = const \ (75\%) \quad (18)$$

Table 1 Characteristics of $H_3(Ph)_3Cor$ floating layers, obtained at different initial surface coverage degrees

c_{face} (c_{edge}), (%)	Nanoagregate type	$c_{i\text{-}face}$-$c_{f.\text{-}face}$ ($\Delta c_{j\text{-}face}$), (%)	$c_{i\text{-}aggr}$, (%)	π_i-π_f, (mN/m)	A_{mol}, (nm^2)	n	D_{aggr} (S_{aggr}) [$V_{aggr\text{-}max}$] nm, nm^2, nm^3	ψ_{min} -ψ_{max}, (°)	r, (nm)	$w_{in\text{-}M}/A_{mol}$, (%)	$w_{inter\text{-}M\text{-}i}$, ($nm^2$)	d_i, (nm)	B, (m/N)
4.3 (2.7)	Monolayers M_{face}	17–22 (5)	68	0.1–0.4[a]	6.39	14	10.8 (92)	0	1.4	75	2.96	2.3	680
7.6 (4.8)		29–35 (6)	74	0.1–0.4[a]	4.13	24	11.2 (98)	0	0.9	61	1.47	1.8	600
10.9 (6.8)		47–59 (12)	69	0.1–0.6[a]	2.33	40	11.0 (94)	0	0.3	31	1.07	2.3	410
17.5 (10.9)	Monolayers M_{edge}	80–109 (29)	73	0.1–2.2	1.46	20	6.1 (29)	55–90	–	18[b]	0.54	1.1	130
20.7 (13.0)		86–114 (28)	77	0.1–2.2	1.42	40	8.6 (57)	58–90	–	15[b]	0.43	1.2	120
24.0 (15.0)		91–117 (26)	78	0.1–2.2	1.35	53	9.6 (72)	62–90	–	12[b]	0.39	1.3	110
27.2 (17.0)		97–123 (26)	79	0.1–2.2	1.31	69	10.7 (90)	66–90	–	8[b]	0.34	1.3	100
37.1 (23.2)	Bilayers M_{bi}	123–147 (24)	83	0.1–2.1	1.08	101	8.3 (54) [173]	–	–	–	0.2	0.8	80
43.3 (27.1)		122–144 (22)	84	0.1–1.9	1.10	106	8.7 (59) [189]	–	–	–	0.2	0.8	90
49.5 (30.9)		133–168 (35)	82	0.1–2.2	0.98	109	8.3 (54) [173]	–	–	–	0.2	0.9	100
61.9 (38.7)		145–174 (29)	84	0.0–1.9	0.92	119	8.3 (55) [176]	–	–	–	0.2	0.8	90
92.8 (58.0)	Tetralayer M_{tetra}	229–267 (38)	81	0.0–2.2	0.57	202	6.1 (29) [186]	–	–	–	0.1	0.7	70

$C = 1.2 \times 10^{-4}$ M, layer compression speed is $v = 2.3$ sm^2 min^{-1}. c_{face} is the initial surface coverage degree. $c_{i\text{-}face}$ and $c_{f\text{-}face}$ are the current surface coverage degrees at the initial and final points of the stable state, respectively. $\Delta c_{j\text{-}face}$ is the state existence region with respect to the current surface coverage degree. $c_{i\text{-}aggr}$ is the degree of surface coverage with M-aggregates at the initial point of the stable state. π_i - π_f, ($\Delta\pi$) is the pressure region, in which the stable state exists. A_{mol} is the surface area per molecule in a nanoaggregate. n is the aggregation number. D_{aggr}, S_{aggr}, and $V_{aggr\text{-}max}$ are the diameter, surface area, and maximum value of volume of a nanoaggregate. ψ_{min} is the minimum tilt of molecules in stacks ("dry" aggregates). $w_{in\text{-}M}$ and $w_{inter\text{-}M\text{-}i}$ are the contents of water in M-aggregates and between them (per molecule) at the initial point of the stable state. r is the average distance between molecule in an aggregate. d_i is the distance between the nanoaggregates at the initial point of the stable state. B is the compressibility of the layer

[a] The length of the region is approximate (due to experimental limitations)

[b] Calculated for vertical position of the molecules

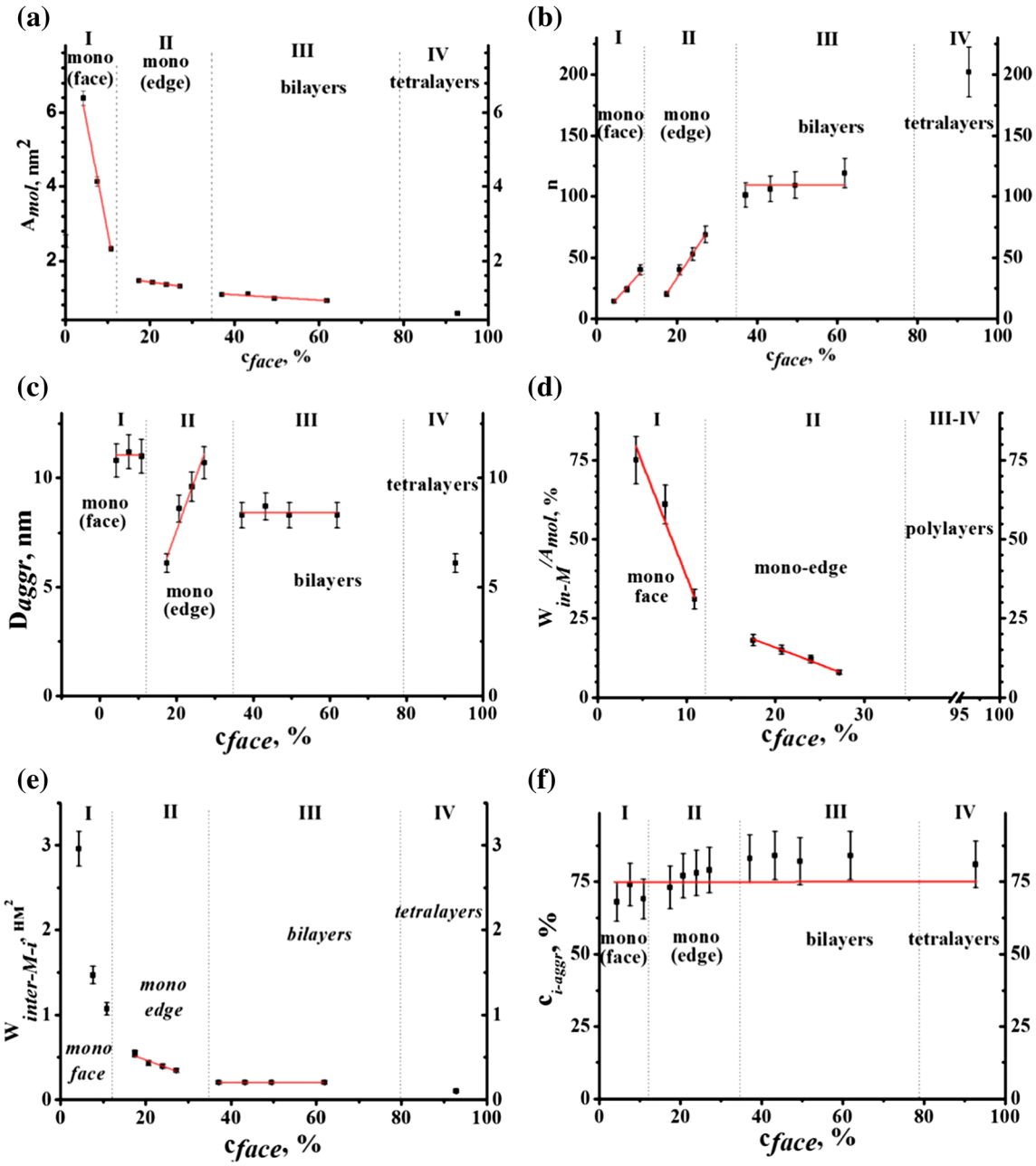

Fig. 4 Dependencies of the surface area per molecule in *M*-aggregate (A_{mol}) (**a**), the aggregation number (n) (**b**), the diameter of *M*-nanoaggregates (D_{aggr}) (**c**), the content of water in nanoaggregates ($w_{in\text{-}M}/A_{mol}$) (**d**), the content of water between nanoaggregates (per molecule, $w_{inter\text{-}M\text{-}i}$) (**e**), and the degree of surface coverage with *M*-aggregates ($c_{i\text{-}aggr}$) (**f**) on the initial surface coverage degree. For plots **e** and **f**, the value determined at the initial point of the stable state. *I*—monolayers (face-on); *II*—monolayers (edge-on); *III*—bilayers; *IV*—tetralayers

For M_{bi} 3D layers:

$$n = const\ (109) \tag{19}$$

$$B = const\ (90\ \text{m/N}) \tag{20}$$

$$D_{aggr} = const\ (8.4\ \text{nm}) \tag{21}$$

$$c_{i-aggr} = const\ (75\%) \tag{22}$$

$$w_{inter\ M-i} = const\ (0.2\ \text{nm}) \tag{23}$$

The resultant dependencies (4–23) can be used to determine the constants, which characterize floating *M*-layers, and these constants are independent of layer formation conditions, such as the maximum and minimum diameters of nanoaggregates and the number of molecules therein, the content of water within and between nanoaggregates, and the monolayer compressibility. The results of the study were used to create a passport of $H_3(Ph)_3Cor$ floating layers, i.e., process parameters for their formation and basic characteristics of the layer's stable states (Table 2).

Table 2 Passport of the floating layers of H_3Ph_3Cor (technological parameters of formation and key properties of the first stable state)[a]

Nanoaggregate type	Molecular orientation in *M*-aggregates	Formation conditions, c_{face} (%) (from the model)	Dependencies of layer characteristics on c_{face} (model)	Constants (from the model)
2D, monolayer M_{face}	face-on (in-plane)	$c_{face} \le 11.7$	$n = -2 + 4 \times c_{face}$ $w_{in\text{-}M}/A_{mol} = 110.1–7.2 \times c_{face}$ $c_{i\text{-face}} = -2.8 + 4.5 \times c_{face}$ $r = 2.2–0.2 \times c_{face}$ D_{aggr} = const (11 nm) $c_{i\text{-aggr}}$ = const (75%)	$n^{max} = 45$ $D_{aggr}^{const} = 11$ nm $w_{in\text{-}M}/A_{mol}^{min} = 26\%$ $(c_{i\text{-face}})^{max} = 50\%$ $(c_{f\text{-face}})^{max} = 66\%$
2D, monolayer M_{edge}	edge-on	$12.5 \le c_{face} \le 33.8$	$n = -62 + 5 \times c_{face}$ $D_{aggr} = -2.3 + 0.5 \times c_{face}$ $w_{in\text{-}M}/A_{mol} = 36.8–1.0 \times c_{face}$ $w_{inter\ M\text{-}i} = 0.84–.02 \times c_{face}$ $c_{i\text{-edge}} = 30.7 + 1.1 \times c_{face}$ $c_{f\text{-edge}} = 52.4 + 0.9 \times c_{face}$ $B = 184.0–3.1 \times c_{face}$ $\psi_{min} = 34.89 + 1.14 \times c_{face}$ $c_{i\text{-aggr}}$ = const (75%)	$n^{max} = 107$ $(D_{aggr})^{max} = 14.3$ nm $(w_{in\text{-}M}/A_{mol})^{min} = 3\%$; $(w_{inter\text{-}M\text{-}i})^{min} = 0.16$ nm $(c_{i\text{-edge}})^{max} = 68\%$ $(c_{f\text{-edge}})^{max} = 79\%$ $B^{min} = 80$ mN/m $(\psi_{min})^{max} = 73°$
3D, bilayer	edge-on	$35.8 \le c_{face} \le 76.9$	n = const (109) D_{aggr} = const (8.4 nm) B = const (90 m/N) $c_{i\text{-aggr}}$ = const (75%) $w_{inter\ M\text{-}i}$ = const (0.2 nm^2)	
3D, tetralayer	edge-on	$c_{face} \ge 81.7$	–	–

$C = 1.2 \times 10^{-4}$ M, layer compression speed $v = 2.3$ sm^2 min^{-1}, $t = 20 \pm 1$ °C

[a] See note of Table 1

The schemes illustrating the fragments and main structural characteristics of monolayers with face-on (c_{face} = 4.3%) and edge-on *M*-nanoaggregates (c_{face} = 27.2%) at the initial points of the stable states are shown in Fig. 5.

Using the horizontal lift technique, the LS films of triphenylcorrole were formed from the floating layers produced on the water surface. Figure 6 shows the UV-Vis spectra of $H_3(Ph)_3Cor$ LS films, which were obtained by transferring edge-on poly- (point A on Fig.3a, isotherm 6) and monolayers (Fig. 6b). The number of substrate immersions (k) into the polylayer is 10 (edge-on polylayers) and 77 (edge-on monolayers).

Figure 6 displays the absorption spectrum of $H_3(Ph)_3Cor$ ($C = 3.6 \times 10^{-5}$ M) solution in CH2Cl2 (1, red lines). This spectrum is typical for free base porphyrins, i.e., has intense Soret band at 415 nm, and weak *Q* bands. The absorbance at these bands is linear on the bulk concentration of the corrole (within the range from 4×10^{-6} M to 4×10^{-5} M), indicating that $H_3(Ph)_3Cor$ exists in the monomeric form. As compared to the monomer solution, the UV-Vis spectra of the films (2, blue lines) demonstrate a red shift of main bands and the long-wavelength shoulder. In the films, 424- and 421-nm peaks are clearly narrower than those

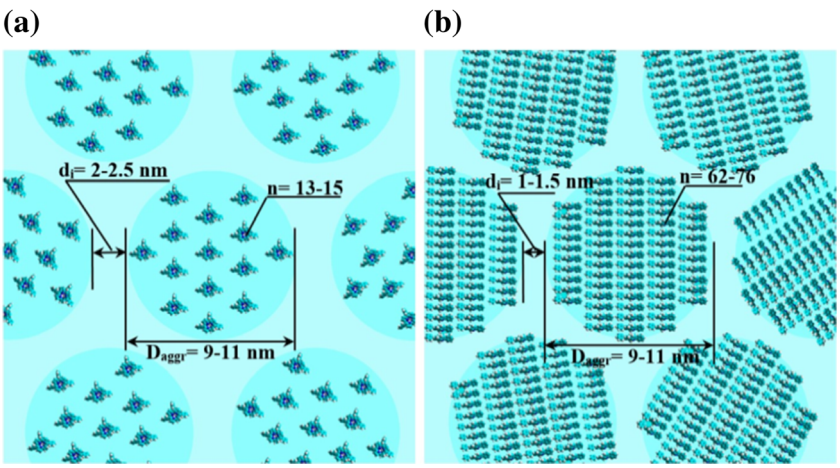

Fig. 5 Schematic representation of fragments of the structure of floating layers of triphenylcorrole with face-on (c_{face} = 4.3%) (**a**) and edge-on (c_{face} = 27.2%) (**b**) *M*-nanoaggregates at the initial points of the stable states

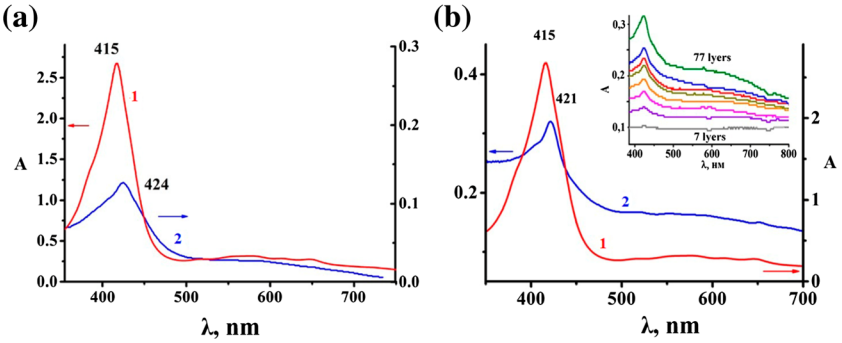

Fig. 6 **a** Absorption spectra of the $H_3(Ph)_3Cor$ ($C = 3.6 \times 10^{-5}$ M) solution in CH2Cl2 (*1*) and its LS films (10 edge-on polylayers) (*2*). The floating layers were transferred onto a solid support by dips at $\pi_{tr} = 6$ mN/m (*point A* on Fig.3a, layer state—"edge-on tetralayer-polylayer"). **b** Absorption spectra of the H_3Ph_3Cor ($C = 3.6 \times 10^{-5}$ mol/l) solution in CH_2Cl_2 (*1*) and its LS films (77 edge-on monolayers) (*2*). *Inset* indicates the absorption spectra of LS films (7, 28, 35, 42, 49, 63, 70, and 77 edge-on monolayers) [21]

observed with the solution. Such a behavior can be associated with the formation of small-sized *J*-aggregates in the films [34–37].

4 Conclusions

In summary, stable floating nanostructured *M*-mono-, bi-, and tetralayers of 5,10,15-triphenylcorrole were obtained. The main characteristics of their structure and properties, and conditions for their formation were determined. It was found that, at this concentration of triphenylcorrole solution in methylene chloride ($C = 1.2 \times 10^{-4}$ M) and this layer compression speed ($v = 2.3$ cm^2/min^{-1}), triphenylcorrole forms nanostructured face-on and edge-on monolayers, the range of initial surface coverage degrees being quite extensive: $4 \le c_{face} \le 33.8\%$. Models of *M*-monolayers were constructed (Eqs. 1, 2, 4–18). If c_{face} is increased to 35.8%, bilayers are formed, and if $c_{face} \ge 81.7\%$, then tetralayers are formed. It was found that the compound's floating layers are characterized by an unchanged degree of surface coverage with 2D and 3D nanoaggregates at the initial point of the stable state (75%). It is important to note that stability of layers with bilayered 3D nanoaggregates is high. The layers are formed within a large range of initial surface coverage degrees (c_{face} from 35.8 to 76.9%). The size of such nanostructures (8.4 nm), the number of molecules in them (109), the distance between them at the initial point of the stable state (0.2 nm^2), and the compressibility of the layer (90 m/N) are independent of the initial surface coverage degree. The first model of a floating bilayer of a macroheterocyclic compound (Eqs. 3, 19–23) were constructed. A passport of 5,10,15-triphenylcorrole floating layers was created. LS films of the corrole were formed from nanostructured floating polylayers produced on the water surface. Comparing the spectra of LS films and solutions shows that small-sized *J*-aggregates are formed in films.

Acknowledgements The work is partially supported by the Russian Scientific Foundation (Project 14-23-00204, formation of polymolecular layers and films) and the Ministry of Education and Science of the Russian Federation (state assignment for the ISUCT, study of the monolayers).

References

1. St. Denis, T. G., Huang, Y.-Y., & Hamblin, M. R. (2013). Cyclic tetrapyrroles in photodynamic therapy: the chemistry of porphyrins and related compounds in medicine. In K. M. Kadish, K. M. Smith, & R. Guilard (Eds.), *Handbook of Porphyrin Science* (Vol. 27, pp. 255–301). Singapore: World scientific.
2. Paolesse, R. (2014). Synthesis and modifications of porphyrinoids. *Topics in Heterocyclic Chemistry, 33*, 1–34.
3. Pawlicki, M., & Latos-Grazyński, L. (2015). Aromaticity switching in porphyrinoids. *Chemistry, an Asian Journal, 10*(7), 1438–1451.
4. Lash, T. D. (2013). Carbaporphyrins and related systems. synthesis, characterization, reactivity and insights into porphyrinoid aromaticity. In K. M. Kadish, K. M. Smith, & R. Guilard (Eds.), *Handbook of Porphyrin Science* (Vol. 16, pp. 1–329). Singapore: World scientific.
5. Aggarwal, A., Qureshy, M., Johnson, J., et al. (2011). Responsive porphyrinoid nanoparticles: development and applications. *Journal of Porphyrins and Phthalocyanines, 15*(5–6), 338–349.
6. Samaroo, D., Perez, E., Aggarwal, A., Wills, A., & O'Connor, N. (2014). Strategies for delivering porphyrinoidbased photosensitizers in therapeutic applications. *Therapeutic Delivery, 5*(7), 59–872.
7. Goslinski, T., & Piskorz, J. (2011). Fluorinated porphyrinoids and their biomedical applications. *Journal of Photochemistry and Photobiology C Photochemistry Reviews, 12*(4), 304–321.
8. Mironov A (2013) Transition metal complexes of porphyrins and porphyrinoids. In: Kadish KM, Smith KM, Guilard R (eds) *Handbook of Porphyrin Science*. World scientific. Singapore., 18(85), pp 303–413.
9. Mack, J. (2013). The effect of structural modifications on the properties of porphyrinoids. In K. M. Kadish, K. M. Smith, & R. Guilard (Eds.), *Handbook of Porphyrin Science* (Vol. 23, pp. 281–371). Singapore: World Scientific.
10. Stillman, M. J. (2013). Theoretical aspects of the optical spectroscopy of porphyrinoids. In K. M. Kadish, K. M. Smith, & R. Guilard (Eds.), *Handbook of Porphyrin Science* (Vol. 14, pp. 461–524). Singapore: World Scientific.
11. Berezin, D. B., & Krest'yaninov, M. A. (2014). Structure of porphyrin H-associates, inverted porphyrinoids, and corroles with N,N-dimethylformamide. *Journal of Structural Chemistry, 55*(5), 822–830.

12. Paolesse R (2014) Applications of porphyrinoids. In: *Topics in heterocyc. Chemistry.* Springer, Berlin, 184.
13. Berezin D. B. (2012). *N-Substituted porphyrinoids: structure, spectroscopy, reactivity.* LAP Lambert Academic Publishing, 64.
14. Valkova, L., Menelle, A., Borovkov, N., Erokhin, V., Pisani, M., et al. (2003). Small-angle X-ray scattering and neutron reflectivity studies of Langmuir–Blodgett films of copper tetra-tert-butyl-azaporphyrines. *Journal of Applied Crystallography, 36*, 758–762.
15. Valkova, L. A., Betrencourt, C., Hochapfel, A., Myagkov, I. V., & Feigin, L. A. (1996). Monolayer study of Monensin and Lasalocid in the gas state. *Molecular Crystals and Liquid Crystals, 287*, 269–273.
16. Akopova, O. B., Kotovich, L. N., Bronnikova, A. A., et al. (1998). Polysubstituted triphenylenes with active groups. Molecular parameters, synthesis, structure, and mesomorphism. *Journal of Structural Chemistry, 39*, 376.
17. Topchieva, I. N., Osipova, S. V., Banatskaya, M. I., et al. (1989). Membrane-active properties of block-copolymers of ethylene-oxide and propylene-oxide. *Doklady Akademii Nauk SSSR, 308*(4), 910.
18. Valkova, L. A., Shabyshev, L. S., Feigin, L. A., & Akopova, O. B. (1996). Formation and X-ray diffraction investigation of Langmuir-Blodgett films of liquid crystalline substituted crown esters. *Molecular Materials, 6*(2), 291–298.
19. Maiorova-Valkova, L. A., Koifman, O. I., Burmistrov, V. A., et al. (2015). 2D M-nanoaggregates in Langmuir layers of calamite mesogen. *Protection of Metals and Physical Chemistry of Surfaces, 51*(1), 85–92.
20. Valkova, L., Borovkov, N., Kopranenkov, V., et al. (2002). Some features of the molecular assembly of copper porphyrazines. *Materials Science and Engineering, 22*, 167.
21. Vu, T. T., Maiorova, L. A., Berezin, D. B., & Koifman, O. I. (2016). Formation and study of nanostructured M-monolayers and LS-films of triphenylcorrole. *Macroheterocycles, 9*(1), 73–79.
22. Maiorova LA (2012) Controlled self-assembling of azaporphyrins in 2D- and 3D-nanostructures in Langmuir layers and Langmuir-Blodgett films. D.Sc. (Phys. And math.) dissertation, Ivanovo State University of Chemistry and Technology, Russia.
23. Supramolecular chemistry (2010) In: Kadish KM, Smith KM, Guilard R (eds) *Handbook of Porphyrin Science*, World scientific, Singapore, 1, pp 600.
24. Tortora, L., Pomarico, G., Nardis, S., et al. (2013). Supramolecular sensing mechanism of corrole thin films. *Sensors and Actuators B, 187*, 72–77.
25. Sinha, W., Kumar, M., Garai, A., Purohit, C. S., Som, T., & Kar, S. (2014). Semi-insulating behaviour of self-assembled tin(IV) corrole nanospheres. *Dalton Transactions, 43*(33), 12564–12573.
26. Valkova, L. A., Glibin, A. S., Koifman, O. I., & Erokhin, V. V. (2011). The influence of molecular structure and π-system extent on nano- and microstructure of Langmuir layers of copper azaporphyrins. *Journal of Porphyrins and Phthalocyanines, 15*, 1044–1051.
27. Valkova, L., Borovkov, N., Pisani, M., & Rustichelli, F. (2001). Three-dimensional structure of the copper porphyrazine layers at the air–water interface. *Thin Solid Films, 401*, 267–272.
28. Karlyuk M.V., Krygin Y.Y., Maiorova-Valkova L.A., Ageeva T.A., Koifman O.I. (2013) *Russian Chemical Bulletin, International Edition*, 62, 471–479.
29. Petrova, M. V., Maiorova, L. A., Gromova, O. A., et al. (2014). Nanostructure of Zinc(II) tetraphenylporphyrinate Langmuir M-monolayers formed with diluted solution. *Macroheterocycles, 7*(3), 267–271.
30. Valkova, L., Valli, L., Casilli, S., et al. (2008). Nanoaggregates of copper porphyrazine in floating layers and Langmuir-Schaefer films. *Langmuir, 24*, 4857.
31. Senge, M. O. (2000). Highly substituted porphyrins. In Kadish KM, Smith KM, Guilard R (Eds.), *The porphyrin handbook* 1, (pp. 239–347) Acad., New York.
32. Valkova, L. A., Glibin, A. S., & Valli, L. (2008). Quantitative analysis of compression isotherms of fullerene C60 Langmuir layers. *Colloid Journal, 70*(1), 6–11.
33. Valkova, L., Zyablov, S., Erokhin, V., & Koifman, O. (2010). Nanoaggregates in floating layers of azaporphyrins. *Journal of Porphyrins and Phthalocyanines, 14*, 513–522.
34. Kasha, M. (1963). Energy transfer mechanisms and the molecular exciton model for molecular aggregates. *Radiation Research, 20*, 55–71.
35. de Miguel, G., Hosomizu, K., Umeyama, T., Matano, Y., Imahori, H., Perez-Morales, M., Martin-Romero, M. T., & Camacho, L. (2011). J-aggregation of a sulfonated amphiphilic porphyrin at the air–water interface as a function of pH. *Journal of Colloid and Interface Science, 356*, 775–782.
36. Rubia-Payá, C., de Miguel, G., Martín-Romero, M. T., et al. (2015). UV–Vis reflection–absorption spectroscopy at air–liquid interfaces. *Advances in Colloid and Interface Science, 225*, 134–145.
37. Zhai, X., Zhang, L., & Liu, M. J. (2004). Supramolecular assemblies between a new series of gemini-type amphiphiles and TPPS at the air/water interface: aggregation, chirality, and spacer effect. *Physical Chemistry B, 108*, 7180–7185.